Supplementary Information (SI) for Physical Chemistry Chemical Physics.

Supporting Information

Using an aromatic linker to optimize charge-resonance states, photodimerization and reversibility in covalent anthracene dimers

Kevin Lam(1), Robert J. Dillon(1)(2), Abel C. Conill(3)*, Tomohiko Nishiuchi(4),
Takashi Kubo(4)*, Rabih O. Al-Kaysi(5), David Casanova(6), Christopher J. Bardeen(1)*

(1)Department of Chemistry
University of California, Riverside
Riverside, CA 92521, USA

(2) U.S. Army Combat Capabilities Development Command, Army Research Laboratory
2800 Powder Mill Rd
Adelphi, MD 20783, USA

(3)Multiverse Computing, 20014 Donostia, Euskadi, Spain

(4)Department of Chemistry, Graduate
School of Science, Osaka University,
Toyonaka, Osaka, Japan

(5)College of Science and Health Professions-3124,
King Saud bin Abdulaziz University for Health Sciences, and King Abdullah International
Medical Research Center (Nanomedicine), Ministry of National Guard Health Affairs, Riyadh
11426, (Kingdom of Saudi Arabia)

(6)Donostia International Physics Center (DIPC) 20018, Donostia, Euskadi, Spain
ǂIKERBASQUE – Basque Foundation for Science, 48009, Bilbao, Euskadi, Spain

Table of Contents for Supporting Information Figures

Materials | Methods | Synthesis of bi(anthracene-9,10-dimethylene)

Materials:

All organic solvents employed in the synthesis of this molecule were of reagent grade, while spectroscopic grade solvents were used in their as-received form. Paraformaldehyde $[CH_2O]_n$ (>90%), Anthracene (97%), Glacial Acetic Acid, and Sodium Iodide (99%) were procured from TCI America and used as received. HCl gas was generated by adding concentrated H_2SO_4 to NaCl.

Methods:

Proton and carbon nuclear magnetic resonance (^1H and ^{13}C NMR) spectra were acquired at a temperature of 298 K using a JEOL spectrometer operating at 400 MHz. Proton chemical shifts were reported in parts per million (ppm, δ) with DMSO-d6 serving as the reference at δ 2.50 ppm. J values were expressed in hertz (Hz). Carbon chemical shifts were also reported in ppm (δ) with DMSO-d6 serving as the reference at δ 39.52 ppm. Complete proton decoupling was applied during ^{13}C NMR experiments which was collected at 101 MHz. A 25% (v/v) mixture of DMSO-d6 in CCl_4 was employed instead of pure DMSO-d6 to enhance solubility of the analyte and prevent the solution from freezing. Abbreviations were used to describe peak splitting patterns: s = singlet, d = doublet, dd = doublet of doublet, ddd = doublet of doublet of doublet, dt = doublet of triplets, tt = triplet of triplets, m = multiplet. Melting points (uncorrected) were determined using a 1101D Mel-Temp digital melting point apparatus.

Synthesis:

Bi(anthracene-9,10-dimethylene)

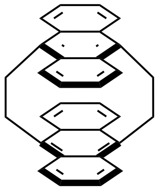

The following reaction schemes (Scheme S1 & Scheme S2) were adopted:

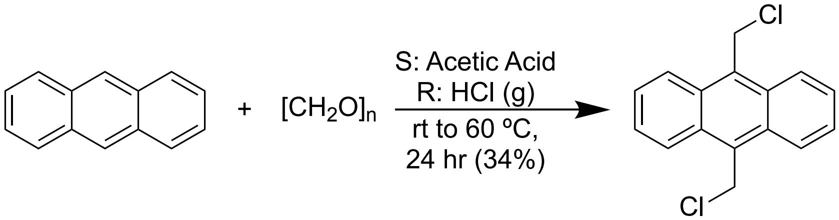

Scheme S1. Synthesis of 9,10-bis(chloromethyl)anthracene.

In a 150 ml flat-bottom flask, 30 ml of glacial acetic acid and paraformaldehyde (4.0 g, 0.13 mol) were added. The mixture was cooled over an ice/water bath and dry HCl was bubbled through until the paraformaldehyde dissolved. Anthracene (4.0 g, 0.022 mol) were added and stirred while allowing the reaction mixture to slowly warm to room temperature. The reaction mixture was stirred overnight (~ 24 hours) at 60 ºC until the white anthracene was replaced with the orange/yellow product. The reaction mixture was cooled over ice/water and suction filtered. The crude product was recrystallized from toluene to obtain yellow-orange needle-like crystals (2.11 grams) with a 34% yield and a melting point of 228-232 °C.

^{1}H NMR (400 MHz, DMSO-D_6) δ 8.51 (dd, J = 6.8, 3.2 Hz, 4H), 7.72 (dd, J = 6.9, 3.1 Hz, 4H), 5.87 (s, 4H) (**Figure S1**)

^{13}C NMR (101 MHz, DMSO-*D6*) δ 130.68, 129.23, 126.76, 124.73 (**Figure S2**)

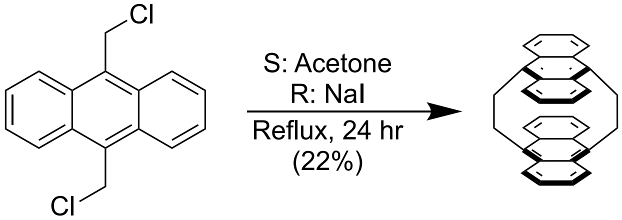

Scheme S2. Synthesis of bi(anthracene-9,10-dimethylene).

The following synthesis was accomplished following the method described by Golden[1] with slight modification. A recrystallized sample of 9,10-bis(chloromethyl)anthracene (0.8g, 0.0029 mol) was gently mixed with NaI (1 g, 0.0066 mol). Into a 100 ml flat-bottom flask, excess NaI (2.5 g, 0.017 mol) was dissolved in 50 mL of dry acetone. The solution was refluxed gently under an atmosphere of argon gas. The 9,10-bis(chloromethyl)anthracene/NaI powder mixture was slowly added over a period of three hours. The reaction mixture was later allowed to reflux overnight under a blanket of argon gas for 24 hours. The crude product was filtered while the solution was hot. The residue was suspended in water and stirred to dissolve the NaI before suction filtration and washing with acetone. The crude product was recrystallized twice from chloroform to obtain small orange crystals (0.33 grams) with a 22% yield. Further recrystallization was performed to ensure a pure product for spectroscopic measurements.

^{1}H NMR (400 MHz, DMSO-*D6*) δ 7.68 (dd, J = 6.7, 3.2 Hz, 8H), 6.84 (dd, J = 6.7, 3.2 Hz, 8H), 4.14 (s, 8H). (**Figure S3**)

^{13}C NMR (101 MHz, DMSO-*D6*) δ 130.83, 130.39, 124.01, 123.44, 28.16. (**Figure S4**)

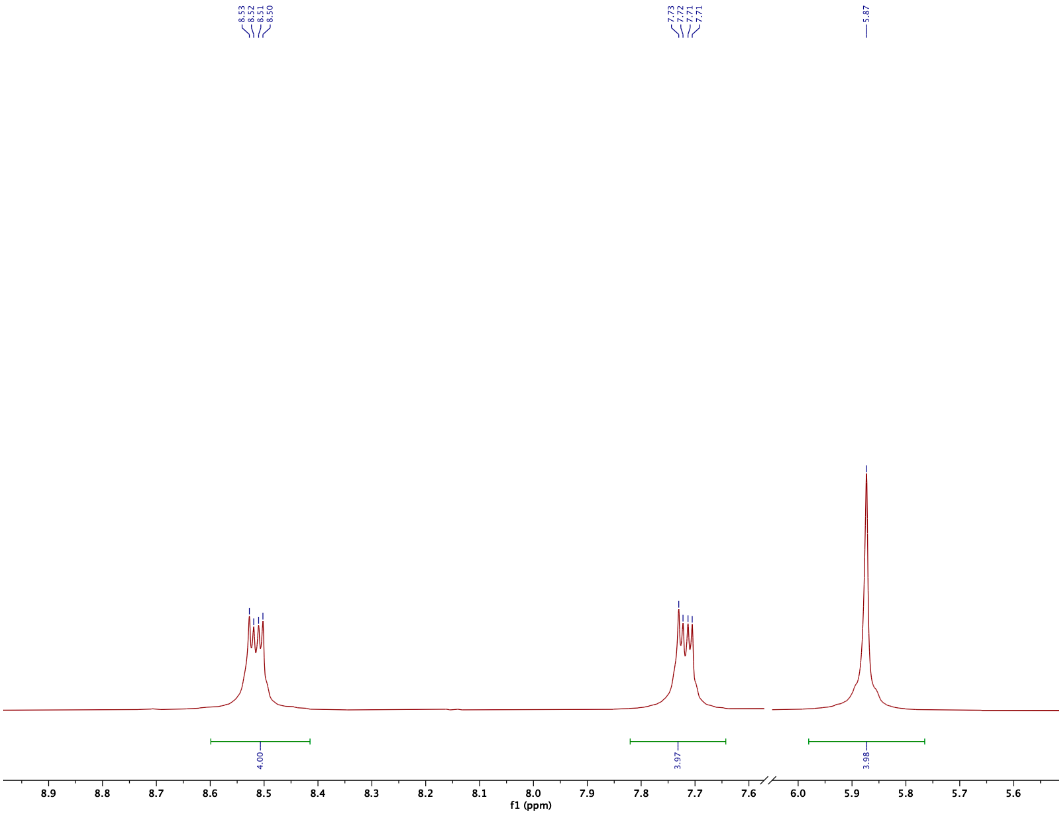

Figure S1. ^{1}H NMR of 9,10-bis(chloromethyl)anthracene in 25% DMSO-d6/ 75% CCl_4 (v/v).

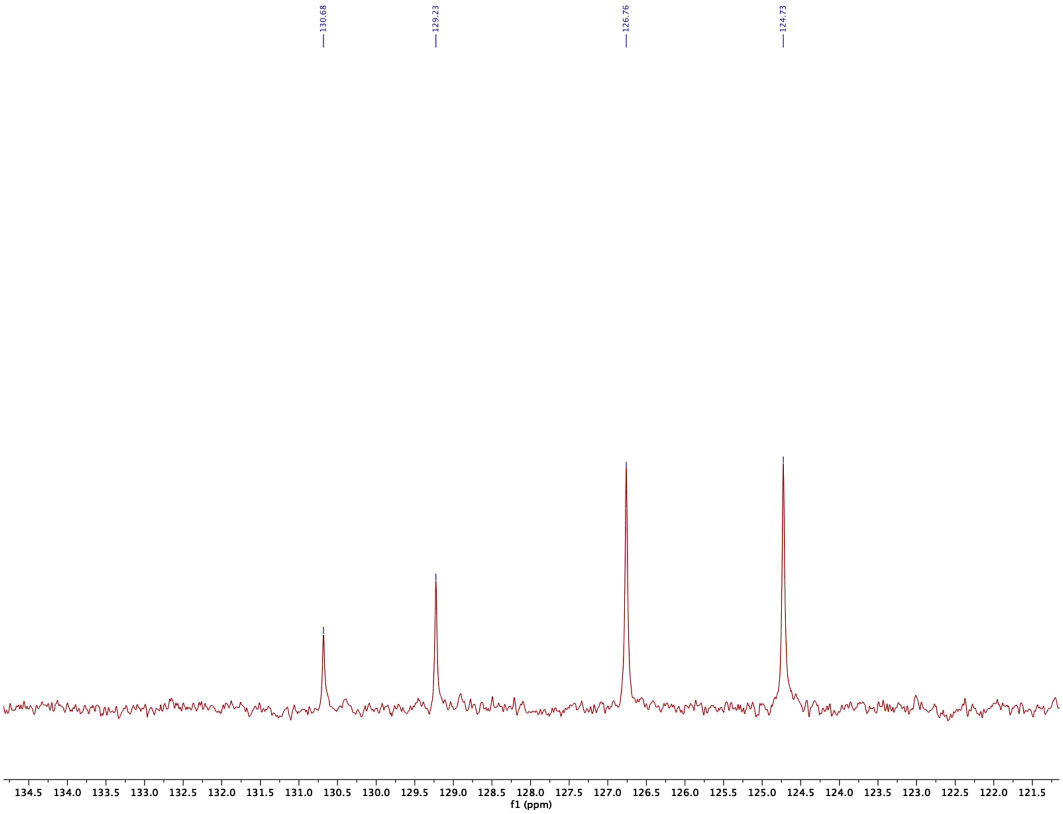

Figure S2. ^{13}C NMR of 9,10-bis(chloromethyl)anthracene in 25% DMSO-d6/ 75% CCl_4 (v/v).

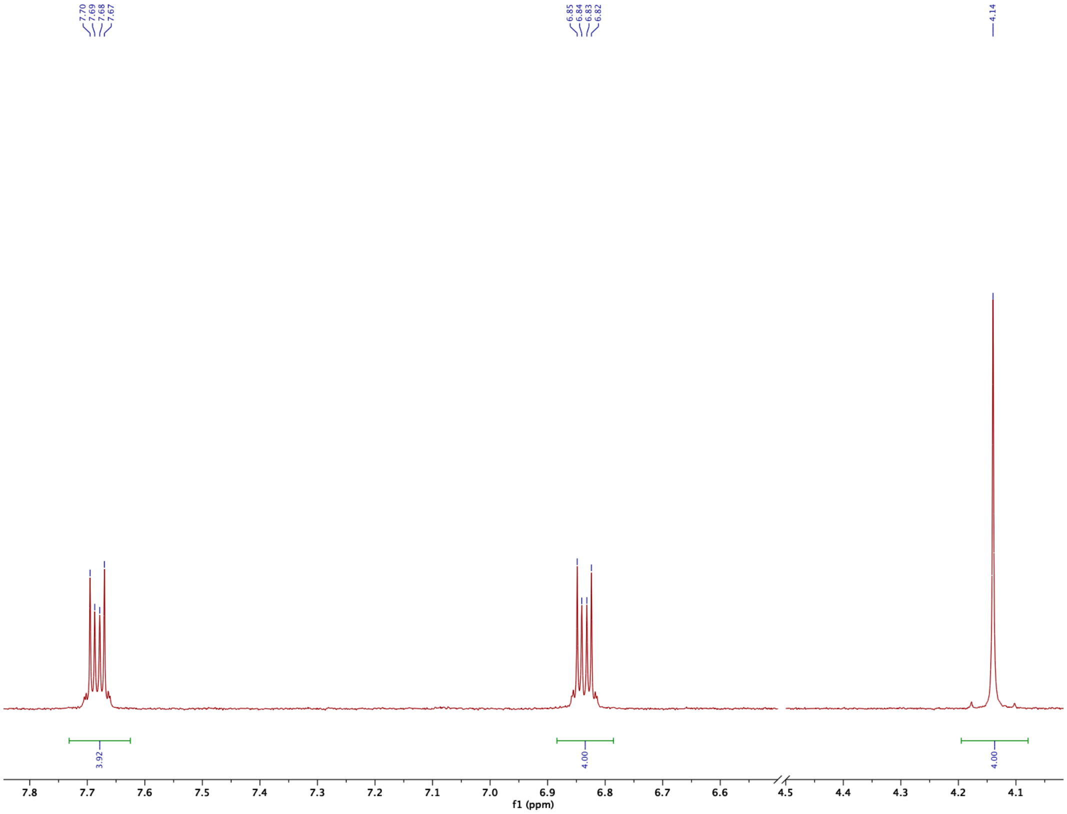

Figure S3. ^{1}H NMR of bi(anthracene-9,10-dimethylene) in 25% DMSO-d6/ 75% CCl_4 (v/v).

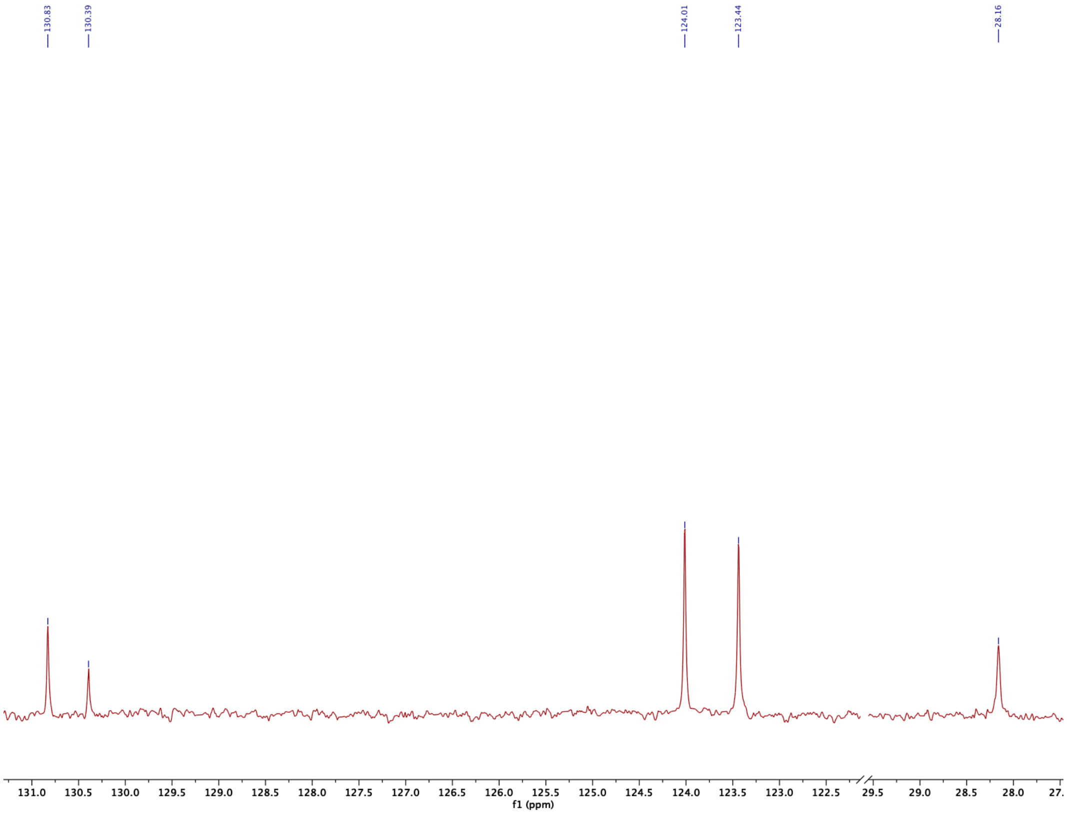

Figure S4. ^{13}C NMR of bi(anthracene-9,10-dimethylene) in 25% DMSO-d6/ 75% CCl_4 (v/v).

Materials | Methods | Synthesis of (-H)mono-benzoannulated [2.2](9,10)anthracenophane and (-OEt)mono-benzoannulated [2.2](9,10)anthracenophane

Materials:

All experiments with moisture- or air-sensitive compounds were performed in anhydrous solvents under nitrogen atmosphere in well-dried glassware. Dried solvents (THF and dichloromethane) were purchased from KANTO CHEMICAL.

Methods:

^{1}H NMR and ^{13}C NMR spectra were recorded on JEOL lambda-500 spectrometer. Column chromatography was performed with silica gel [Silica gel 60N (KANTO CHEMICAL)]. Melting points were measured by using Büchi M-565. Positive APCI-MS spectra were recorded on an Advion expression CMS-L spectrometer and a Bruker micrOTOF II spectrometer.

Synthesis:

(-H)mono-benzoannulated [2.2](9,10)anthracenophane

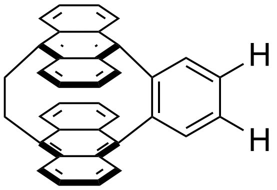

(-H)mono-benzoannulated [2.2](9,10)anthracenophane was synthesized from 9-bromo-10-hydroxymethylanthracene as previously described.[2]

(-OEt)mono-benzoannulated [2.2](9,10)anthracenophane

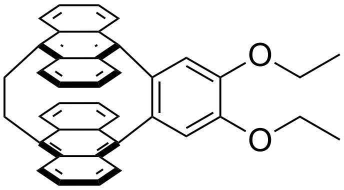

The following reaction schemes (Scheme S3-S5) were adopted:

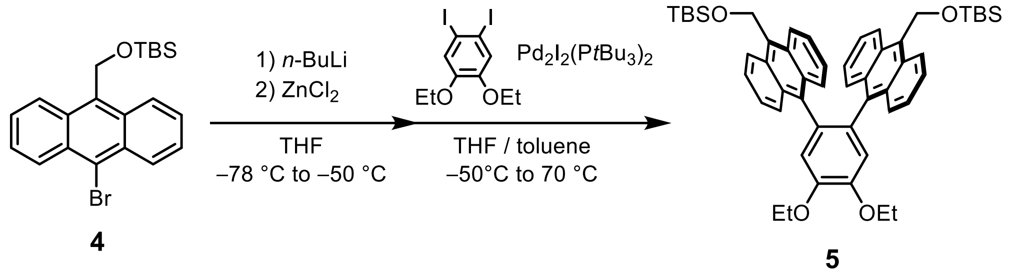

Scheme S3. Synthesis of compound **5**.

To a solution of compound **4**[2] (7.20 g, 17.9 mmol) in THF (30 ml), *n*-BuLi (1.6 M hexane solution, 12.5 ml, 20.0 mmol) was added at −78 °C. After stirring for 1 h at same temperature, a suspension of zinc chloride (3.40 g, 25.0 mmol) in THF (20 ml) was added and stirred at −50 °C. After stirring for additional 1 h, a suspension of 1,2-diethoxy-4,5-diiodobenzene[3] (3.34 g, 7.99 mmol) and $Pd_2I_2(P^tBu_3)_2$ (70 mg, 0.08 mmol) in toluene (25 ml) was added and heated up to 70 °C for 18 h. The reaction was quenched by water. Organic layer was extracted with dichloromethane and washed with brine. After removal of the solvent *in vacuo*, the crude material was subjected to column chromatography on silica gel (hexane:dichloromethane = 2:1) to afford the compound **5** (5.19 g, 6.42 mmol, 80%) as yellow solid. MP: 94-95 °C. MS (APCI): m/z 807.1 [$(M+H)^+$].

^1H NMR (500 MHz, $CDCl_3$) δ 8.03 (d, J = 8.8 Hz, 4H, aromatic proton), 7.96 (d, J = 8.8 Hz, 4H, aromatic proton), 7.22 (s, 2H, aromatic proton), 7.20 (dd, J = 6.5 Hz, J = 1.0 Hz, 4H, aromatic proton), 7.02 (dd, J = 6.5 Hz, J = 1.0 Hz, 4H, aromatic proton), 5.32 (s, 4H, $-SiOCH_2-$ proton), 4.22 (q, J = 7.0 Hz, 4H, $-OCH_2CH_3$ proton), 1.53 (t, J = 7.0 Hz, 6H, $-OCH_2CH_3$ proton), 0.77 (s, 18H, $-CCH_3$ proton), −0.25 (s, 12H, $Si-CH_3$ proton). (**Figure S5**)

^{13}C NMR (125 MHz, $CDCl_3$) δ 147.69, 136.65, 132.17, 130.75, 129.83, 129.41, 128.34, 124.82, 124.00, 123.63, 117.75, 64.57, 57.88, 25.83, 18.22, 14.89 −5.20. (**Figure S6**)

HR-MS (APCI) Calcd. for $C_{52}H_{62}O_4Si_2$ [M^+]: m/z 806.4181, Found: 806.4187.

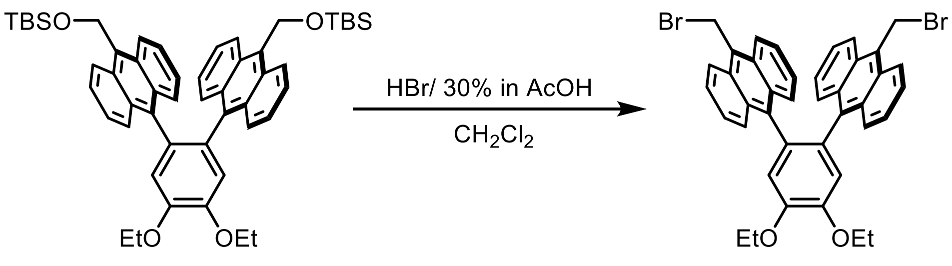

5 **6**

Scheme S4. Synthesis of compound **6**.

To a solution of **5** (3.63 g, 4.50 mmol) in dichloromethane (50 ml) was added HBr (30% acetic acid solution, 2.6 ml) at room temperature. After stirring for 12 h, the reaction was quenched by water. Organic layer was extracted with dichloromethane and washed with brine. After removal of the solvent *in vacuo*, the crude material was washed with diethyl ether to afford the compound **6** (2.81 g, 3.99 mmol, 89%) as yellow solid. Due to its instability, compound **6** was used without silica gel column purification.; MP: 220 °C (dec.). MS (APCI): m/z 625.6 $[(M-Br)^+]$.

^{1}H NMR (500 MHz, CD_2Cl_2) δ 8.04 (d, *J* = 9.0 Hz, 4H, aromatic proton), 7.96 (d, *J* = 9.0 Hz, 4H, aromatic proton), 7.36 (dd, *J* = 6.5 Hz, *J* = 1.0 Hz, 4H, aromatic proton), 7.22 (s, 2H, aromatic proton), 7.13 (dd, *J* = 6.5 Hz, *J* = 1.0 Hz, 4H, aromatic proton), 5.24 (s, 4H, -CH_2Br proton), 4.19 (q, *J* = 7.0 Hz, 4H, -OCH_2CH_3 proton), 1.50 (t, *J* = 7.0 Hz, 6H, -OCH_2CH_3 proton). (**Figure S7**)

^{13}C NMR (125 MHz, CD_2Cl_2) δ 148.49, 138.61, 131.73, 130.41, 129.12, 129.05, 127.63, 126.29, 124.75, 123.29, 117.85, 64.96, 27.92, 15.07. (**Figure S8**)

HR-MS (APCI) Calcd. for $C_{40}H_{32}Br_2O_2$ $[(M+H)^+]$: m/z 708.0825, Found: 708.0825.

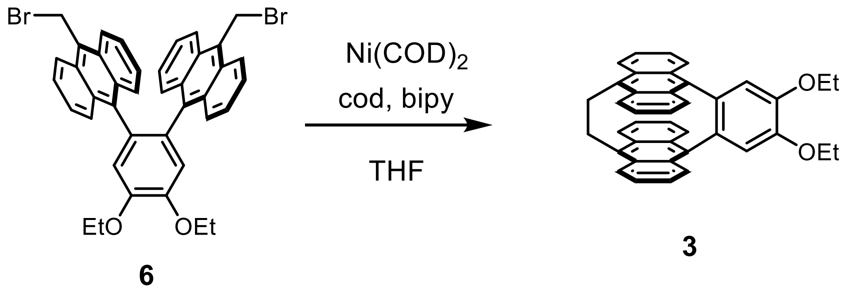

Scheme S5. Synthesis of compound **3**.

Bis(cyclooctadiene)nickel(0) (1.60 g, 5.80 mmol), cyclooctadiene (0.900 ml, 7.30 mmol), and 2,2'-bipyridine (1.14 g, 7.30 mmol) were dissolved in THF (140 ml) and stirred for 1h at 60 °C under absence of light for activation of nickel catalyst. After the activation, this reaction mixture was cooled at −15 °C and a solution of **6** (2.11 g, 3.00 mmol) in THF (70 ml) was added. After stirred for 18 h at −15 °C, the reaction was quenched by 2M hydrochloric acid. The organic layer was extracted with dichloromethane, washed with brine, and dried over $MgSO_4$. After removing organic solvent *in vacuo*, the crude material was subjected to column chromatography on silica gel (hexane : toluene = 1 : 4 to toluene only) to afford the compound **3** (1.19 g, 2.19 mmol, 30%) as a red solid. MP: >300 °C. MS (APCI): *m/z* 545.7 $[(M+H)^+]$.

^1H NMR (500 MHz, $CDCl_3$) δ 8.00 (d, J = 9.0 Hz, 4H, aromatic proton), 7.90 (d, J = 9.0 Hz, 4H, aromatic proton), 7.20 (s, 2H, aromatic proton), 7.18 (dd, J = 6.5 Hz, J = 1.0 Hz, 4H, aromatic proton), 7.04 (dd, J = 6.5 Hz, J = 1.0 Hz, 4H, aromatic proton), 4.21 (q, J = 7.0 Hz, 4H, $-OCH_2CH_3$ proton), 2.74 (s, 4H, $-CH_2$-proton), 1.52 (t, J = 7.0 Hz, 6H, $-OCH_2CH_3$ proton). (**Figure S9**)

^{13}C NMR (125 MHz, $CDCl_3$) δ 147.60, 134.38, 132.50, 129.78, 129.34, 129.21, 128.54, 124.30, 124.08, 123.58, 118.04, 64.52, 14.90, 13.86. (**Figure S10**)

HR-MS (APCI) Calcd. for $C_{40}H_{32}O_2$ $[M^+]$: m/z 544.2397, Found: 544.2400.

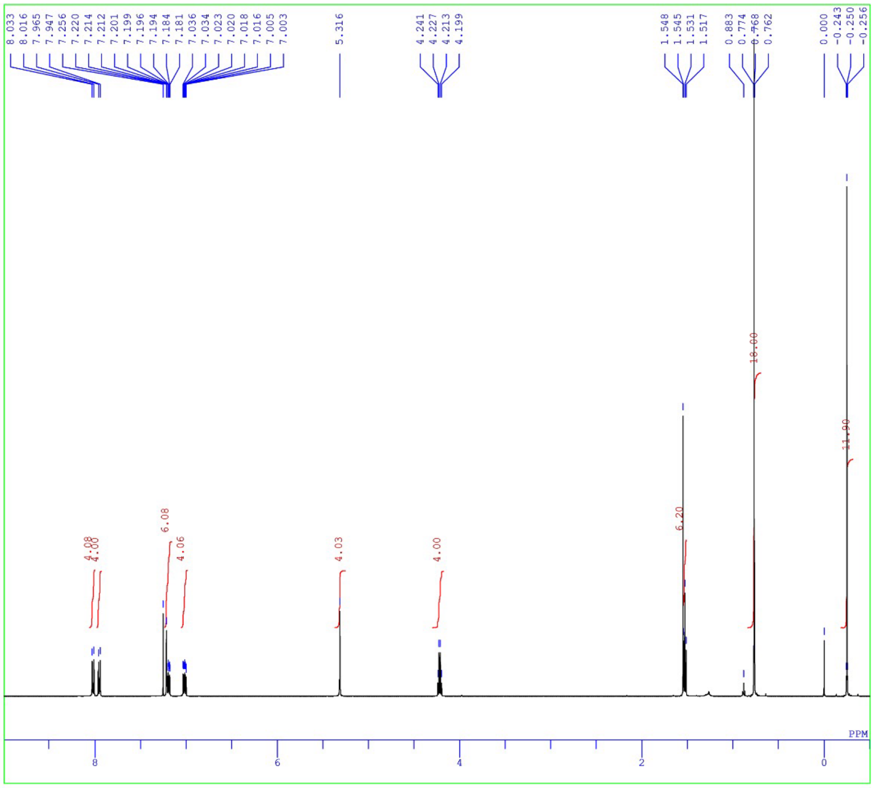

Figure S5. ^{1}H NMR of **5** in CD_2Cl_2.

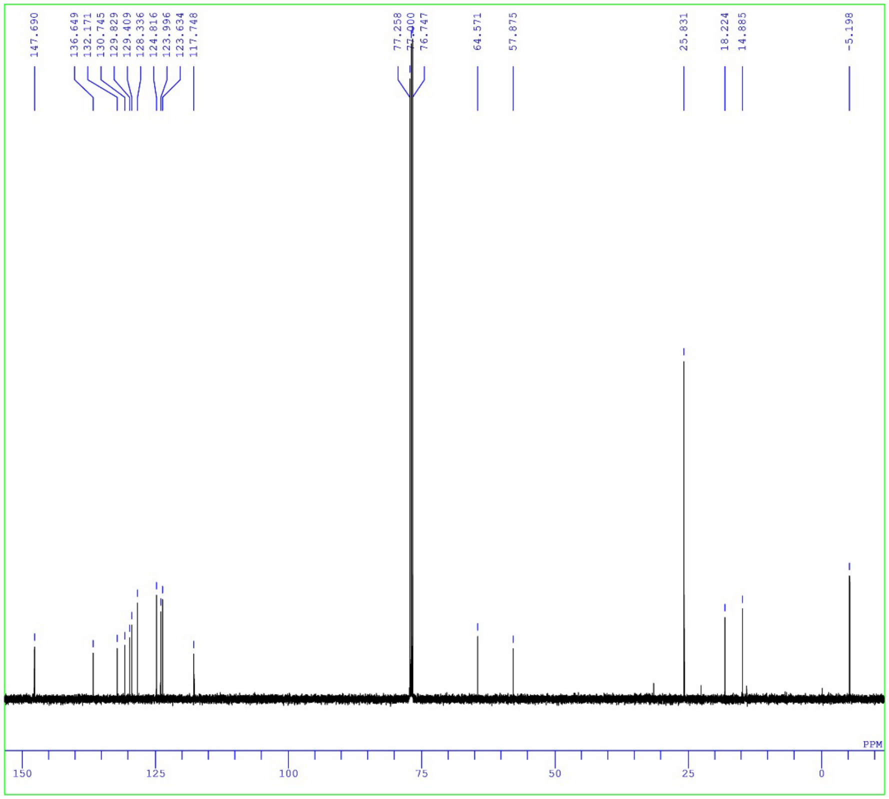

Figure S6. ^{13}C NMR of **5** in CD_2Cl_2.

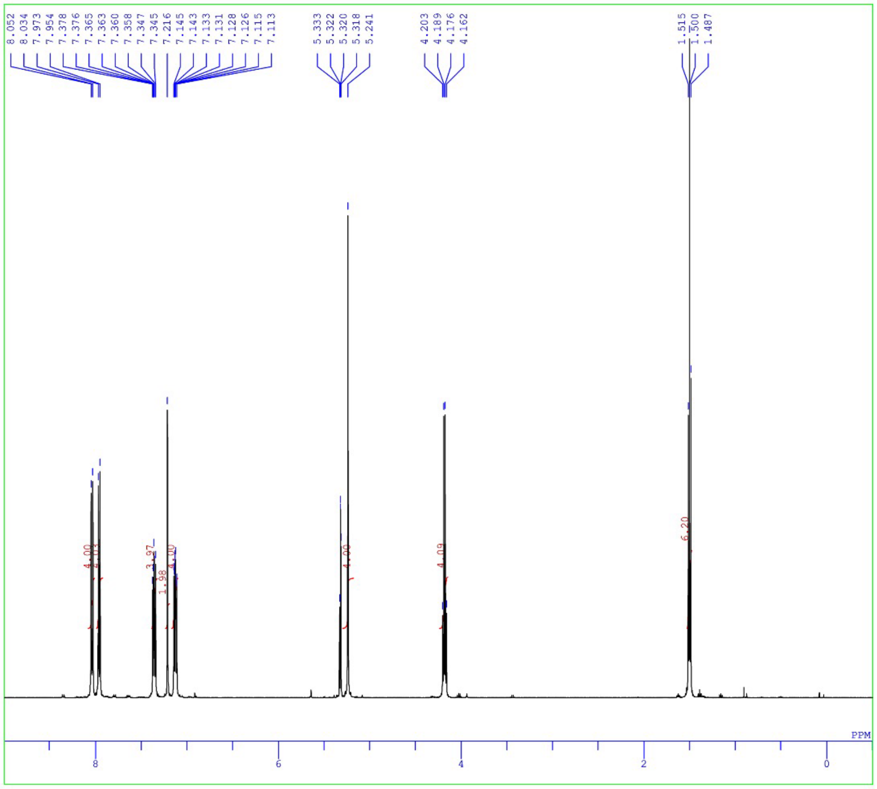

Figure S7. ^{1}H NMR of **6** in CD_2Cl_2.

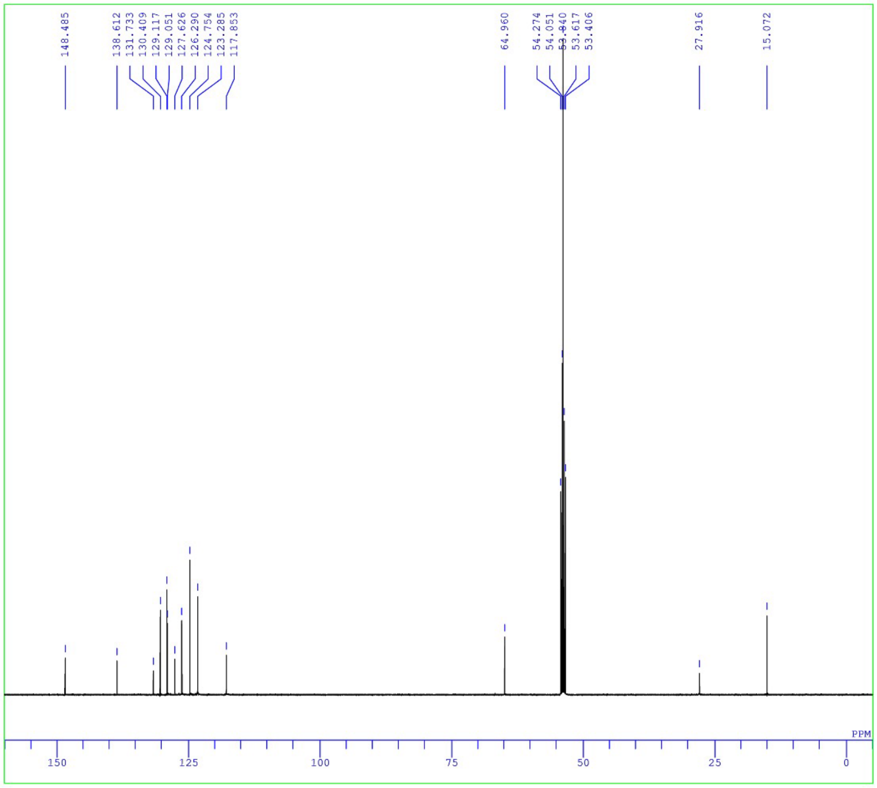

Figure S8. ^{13}C NMR of **6** in CD_2Cl_2.

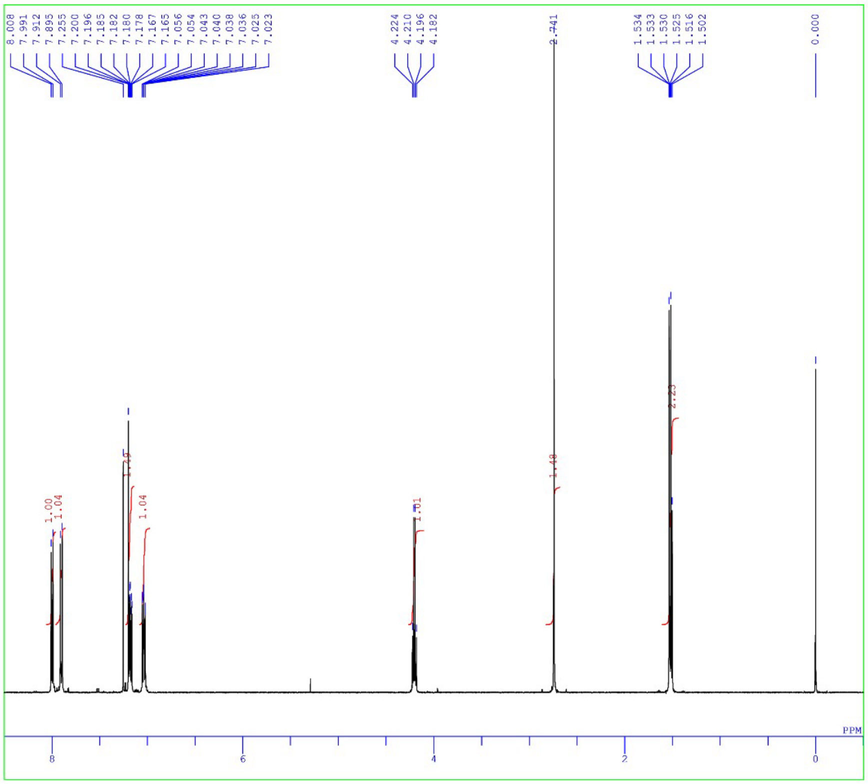

Figure S9. ^{1}H NMR of **3** in CDCl$_3$.

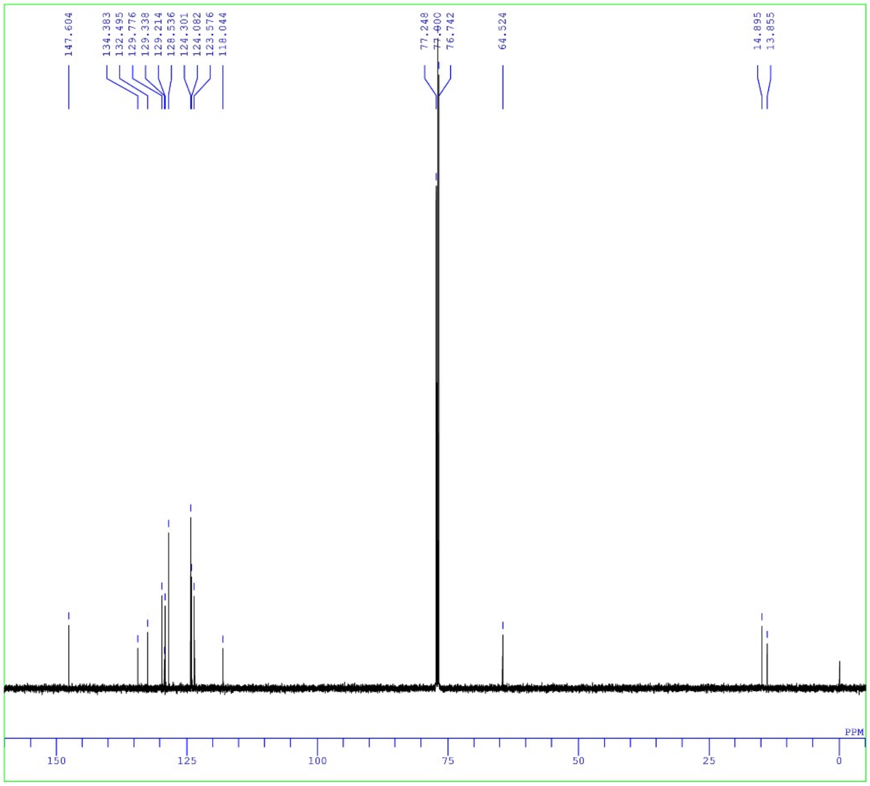

Figure S10. ^{13}C NMR of **3** in CDCl$_3$.

Steady-state UV/Vis Absorption Spectra Measurements:

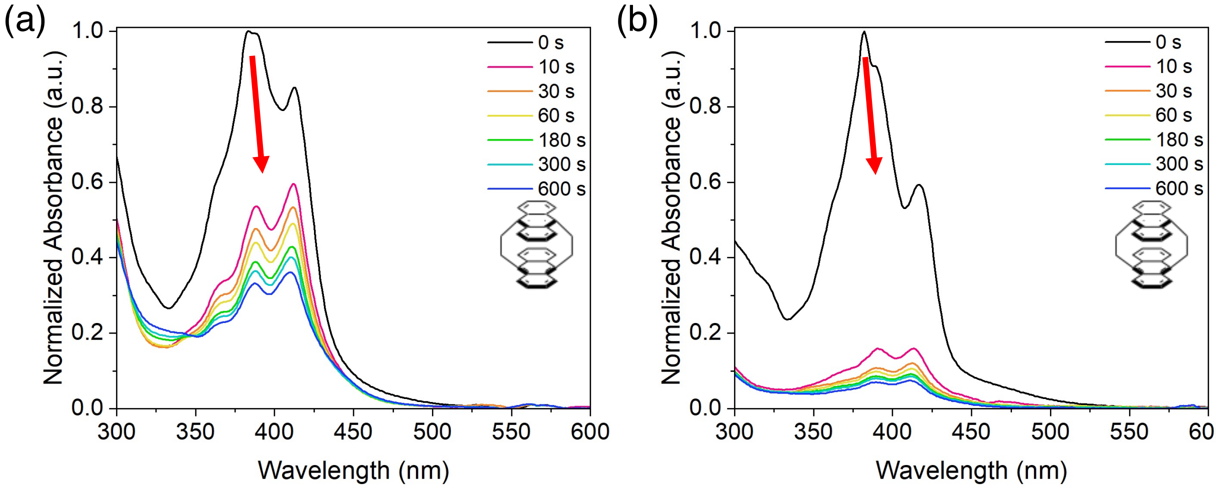

Figure S11. Normalized steady-state absorption spectra measurements of bi(anthracene-9,10-dimethylene) in chloroform after it had undergone (a) one and (b) two purification steps. The decay in absorbance during continuous photolysis at 365 nm (14 mW/cm^2) is shown. Note how an anthracene-like peak remains after extended photolysis and how the amplitude of that peak is proportional to the level of purification.

Single-Crystal X-Ray Structural Determination Measurements:

Crystal data for (-OEt)mono-benzoannulated [2.2](9,10)anthracenophane:
CCDC 2387424. $C_{40}H_{32}O_2$, MW = 544.65, orthorhombic, space group P $2_12_12_1$ (no. 19), a = 9.1458(10), b = 11.4764(14), c = 26.799(3) Å, α = 90°, β = 90°, γ = 90°, V = 2812.8(6) Å^3, Z = 4, D = 1.286 g/cm^3, T = 113 K, Data collection with MoKα radiation (multi-layer mirror monochromated). 15254 measured reflections, 6294 unique reflections; structure solution by direct methods (Shelxs), refinement by full-matrix least squares on F with anisotropic temperature factors for the non-H atoms. Final R1 = 0.0517, wR2 = 0.1013, GOF = 0.990.

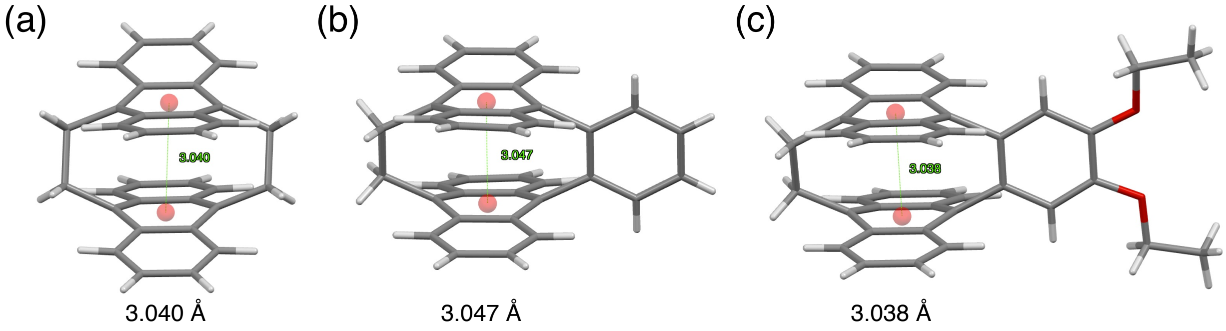

Figure S12. X-ray crystallographic structures of (a) bi(anthracene-9,10-dimethylene), (b) (-H)mono-benzoannulated [2.2](9,10)anthracenophane, and (c) (-OEt)mono-benzoannulated [2.2](9,10)anthracenophane, all showing that the central anthracene ring is within the 4.1 Å distance required for [4+4] photodimerization to proceed. Crystallographic information was taken from the following CCDC deposition numbers: (a) 1103119, (b) 1969048, and (c) 2387424.

Steady-state UV/Vis Absorption Spectra Measurements:

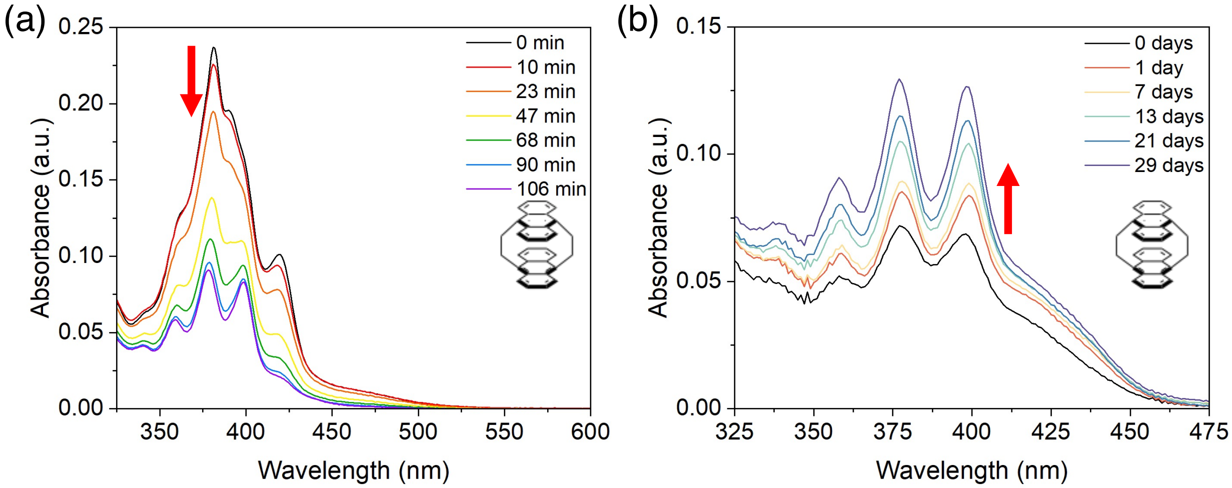

Figure S13. (a) Steady-state absorption spectra measurements of bi(anthracene-9,10-dimethylene) in toluene after heating at 90 °C for an extended period of time, showing heat-induced degradation of the molecule. (b) Absorption measurements tracking the recovery of the degraded product under ambient conditions over the course of a month, revealing that this process is irreversible.

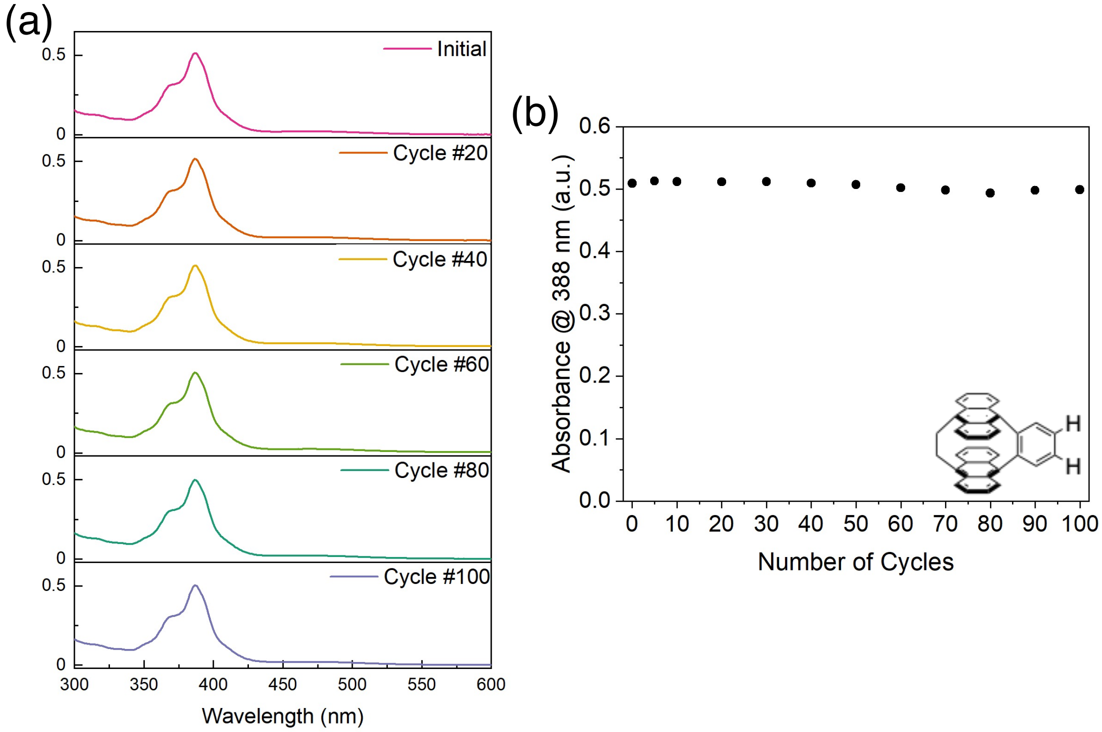

Figure S14. (a) Steady-state absorption spectra measurements of (-H)mono-benzoannulated [2.2](9,10)anthracenophane after numerous cycles of repeated photolysis at 365 nm followed by incubation at 100 ºC for five minutes to regenerate the monomer pair. (b) λ_{max} tracked as a function of cycle number, showing that no degradation of the molecule occurs over one hundred cycles.

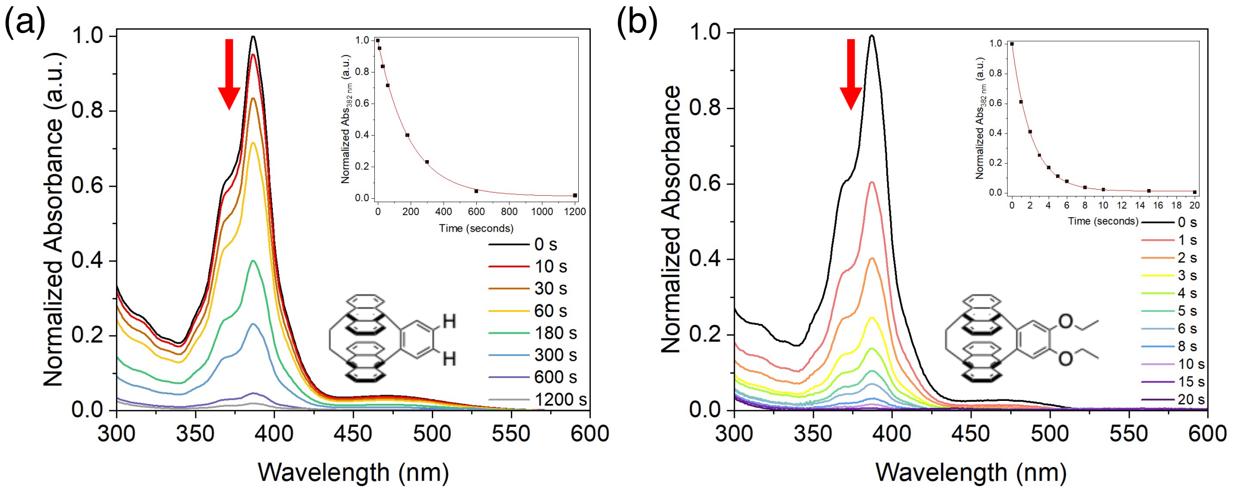

Figure S15. Normalized steady-state absorption spectra of (a) (-H)mono-benzoannulated [2.2](9,10)anthracenophane in chloroform showing the decay in absorbance during continuous photolysis at 532 nm (14 mW/cm^2) and (b) (-OEt)mono-benzoannulated [2.2](9,10)anthracenophane in chloroform showing the decay in absorbance during continuous photolysis at 365 nm (14 mW/cm^2).

Table S1. Estimated photodimerization quantum yields of (-H)mono-benzoannulated [2.2](9,10)anthracenophane (**2**) and (-OEt)mono-benzoannulated [2.2](9,10)anthracenophane (**3**) calculated from the kinetic dimerization rate constant measured at λ_{max} ($k_{382\ nm}$), absorption cross section (σ), and measured light intensity of λ_{ex}.

Molecule	**2**	**2**	**3**
λ_{ex} (nm)	365	532	365
$k_{382\ nm}$ (s^{-1})	0.356 ± 0.006	0.0052 ± 0.0002	0.422 ± 0.030
σ (cm^2)	2.97×10^{-17}	3.73×10^{-19}	3.04×10^{-17}
I ($cm^2\ s^{-1}$)	2.57×10^{16}	3.75×10^{16}	2.57×10^{16}
Φ_{dim}	0.47 ± 0.05	0.83 ± 0.09	0.54 ± 0.07

Density Functional Theory Analysis of Electronic Structures:

Table S2. Vertical excitation energies (ΔE in eV) and oscillator strengths *f*, to low-lying excited singlets at the ground state optimized geometries of **1** and **2** computed at the CAM-B3LYP-D3 level with the cc-pVDZ and the cc-pVTZ (italics) basis. Boldface indicates the bright state (S_B) corresponding to the main absorption band of the spectra.

	molecule **1**		molecule **2**	
state	ΔE	f	ΔE	f
S_1	3.01/*2.94*	0.0000/*0.0000*	2.81/*2.75*	0.0037/*0.0031*
S_2	3.43/*3.39*	0.0001/*0.0000*	3.47/*3.43*	0.0066/*0.102*
S_3	**3.75**/***3.68***	**0.2213**/***0.2076***	3.61/*3.55*	0.0205/*0.0241*
S_4	3.78/*3.73*	0.0000/*0.0000*	**3.78**/***3.71***	**0.2374**/***0.2125***
S_5	3.79/*3.77*	0.0000/*0.0000*	3.97/*3.93*	0.0019/*0.0015*
S_6	4.00/*3.97*	0.0039/*0.0026*	4.10/*4.07*	0.0030*0.0026*

Computed oscillator strengths for the transition to S_1 are quite small in both molecules, consistent with the experimentally observed weak absorption band at longer wavelengths. Notably, the calculated oscillator strength for S_1 in molecule **1** is zero, indicating an optically inactive transition. However, it is important to note that these calculations were performed on a single frozen geometry optimized for the ground state. In reality, thermal fluctuations at room temperature could enable weak transitions to S_1. The calculated state S_2 has larger oscillator strength and significant CT character but does not show the observed energy redshift relative to S_3/S_4 to be assigned to the S_A state.

Table S3. Vertical de-excitation energies (in eV) and oscillator strengths *f*, from the lowest-lying excited singlet at the S_1 (excimer) optimized geometries of **1** and **2** computed at the CAM-B3LYP-D3/cc-pVDZ level.

	molecule **1**		molecule **2**	
state	ΔE	f	ΔE	f
S_1	1.89	0.0000	1.83	0.0009

Table S4. Decomposition of electronic transitions to singlet excited states of **1** and **2** (S_1 excimer geometry) in terms of local excitations (within of each anthracene unit, LE_1 and LE_2) and charge transfer (CT_{12} and CT_{21}) computed at the CAM-B3LYP-D3/cc-pVDZ level.

	molecule **1**				molecule **2**			
state	CT_{12}	CT_{21}	LE_1	LE_2	CT_{12}	CT_{21}	LE_1	LE_2
S_1	0.237	0.237	0.233	0.233	0.238	0.238	0.234	0.234

Table S5. Cartesian coordinates of bi(anthracene-9,10-dimethylene) (**1**) in the ground state optimized at the CAM-B3LYP-D3/cc-pVDZ level.

Atom	X (Å)	Y (Å)	Z (Å)
C	3.079722604	-1.723187198	0.455852064
C	4.247742015	-1.29532643	-0.078126751
C	4.243179544	-0.477426238	-1.231766124
C	3.070804886	-0.120353747	-1.806478965
C	-1.737327744	-0.867387255	-2.320529601
C	-2.851382312	-1.552328799	-1.968942033
C	-2.848061762	-2.369046236	-0.815348405
C	-1.731475922	-2.468018092	-0.055066402
C	0.606783234	-1.844098552	0.410626117
C	0.598631407	-0.210327404	-1.891367351
C	-0.532274944	-0.969814154	-1.572014295
C	-0.529000613	-1.794751373	-0.405713472
C	1.821614258	-1.410049961	-0.1362646
C	1.817308891	-0.578829064	-1.307203396
C	0.438225145	1.085348163	-2.646429867
C	0.458277658	-2.141210449	1.882612508
H	3.102492857	-2.360597494	1.326387453
H	5.187415884	-1.582928879	0.372339445
H	5.17926281	-0.144682858	-1.658041973
H	3.086602445	0.486989359	-2.69825986
H	-1.750948454	-0.243176226	-3.201481966
H	-3.749582231	-1.471782812	-2.564528631
H	-3.743119472	-2.907844774	-0.538554797
H	-1.740042446	-3.091213845	0.826623236
H	1.413602275	1.527888023	-2.812551898
H	0.000314044	0.932363617	-3.632876448
H	1.437419401	-2.149737312	2.347871431
H	0.030481727	-3.12803097	2.059027607
C	-0.438225145	-1.085348163	2.646429867
C	-0.598631408	0.210327404	1.891367351
C	0.532274944	0.969814151	1.572014294
C	1.737327745	0.867387249	2.320529597
C	2.851382314	1.552328791	1.968942028
C	2.848061764	2.369046227	0.815348399
C	1.731475924	2.468018086	0.055066398
C	0.529000613	1.79475137	0.40571347
C	-0.606783235	1.844098552	-0.410626117
C	-1.821614259	1.410049963	0.136264601
C	-3.079722605	1.723187204	-0.45585206
C	-4.247742017	1.295326439	0.078126756
C	-4.243179546	0.477426247	1.23176613
C	-3.070804888	0.120353752	1.806478968
C	-1.817308893	0.578829066	1.307203398
H	-3.086602447	-0.486989353	2.698259864
H	-5.179262812	0.144682869	1.65804198
H	-5.187415886	1.58292889	-0.372339438
H	-3.102492858	2.3605975	-1.326387449
C	-0.458277658	2.141210449	-1.882612508
H	-1.4374194	2.149737314	-2.347871431
H	-0.030481725	3.12803097	-2.059027607
H	1.740042447	3.091213839	-0.82662324
H	3.743119475	2.907844763	0.53855479
H	3.749582234	1.471782801	2.564528624
H	1.750948454	0.24317622	3.201481962
H	-1.413602274	-1.527888023	2.812551901
H	-0.000314042	-0.932363617	3.632876447

Table S6. Cartesian coordinates of (-H)mono-benzoannulated [2.2](9,10)anthracenophane (**2**) in the ground state optimized at the CAM-B3LYP-D3/cc-pVDZ level.

Atom	X (Å)	Y (Å)	Z (Å)
C	-0.19343638	0.680180018	-2.248455439
C	0.647868617	1.734048925	1.256865239
C	0.721278057	1.725700857	-0.1703308
C	-1.709278349	1.300932744	1.14269503
C	-1.640915083	1.30952928	-0.289276245
C	-0.390956939	1.328732041	-0.917396688
C	-0.524091939	1.312177574	1.893526049
C	1.82012761	2.071132091	1.988965313
H	1.771882289	2.088366232	3.067515983
C	-0.439117911	0.659266791	3.25017561
H	-1.436383952	0.400022378	3.587863639
H	-0.021163859	1.326854408	4.00373609
C	1.968070581	2.026507565	-0.785170826
H	2.031402881	1.991144259	-1.862672116
C	-0.372802643	1.330969341	-3.456969486
H	-0.660420934	2.37354734	-3.454132164
C	-2.851866507	1.213937718	-1.030996806
H	-2.792735716	1.19050641	-2.108894661
C	-0.184903641	0.665435972	-4.658778347
H	-0.328745825	1.190180153	-5.592970262
C	-2.999032999	1.227751738	1.742415144
H	-3.076789557	1.240813734	2.818945083
C	2.973650775	2.403750267	1.36265795
H	3.843999754	2.683366167	1.939427815
C	3.050829103	2.372550658	-0.049815284
H	3.982860481	2.616779171	-0.539539619
C	-4.130705064	1.202702014	0.998170066
H	-5.096392946	1.187588248	1.483877218
C	-4.05695191	1.190263185	-0.414278256
H	-4.965806732	1.15416832	-0.998472726
C	0.19348412	-0.680149012	-2.248453446
C	-0.647867003	-1.733899252	1.256862215
C	-0.721271854	-1.725535642	-0.170334038
C	1.709334012	-1.301076772	1.142703339
C	1.640970855	-1.309657596	-0.28927012
C	0.391011891	-1.328704054	-0.917396737
C	0.524139786	-1.3121806	1.893535574
C	-1.820174513	-2.070820089	1.988958587
H	-1.771933943	-2.088060067	3.067509951
C	0.43912191	-0.659299648	3.2501981
H	1.436374841	-0.400110379	3.587962101
H	0.021081244	-1.326878303	4.003719043
C	-1.968103306	-2.026166025	-0.78518145
H	-2.031426215	-1.990787266	-1.862683193
C	0.372789627	-1.330956313	-3.456966573
H	0.660394064	-2.373538185	-3.45412739
C	2.851934203	-1.21423626	-1.030994954
H	2.792803493	-1.19079735	-2.108892483
C	0.184849602	-0.665436687	-4.658776666
H	0.328650314	-1.190194557	-5.592967279
C	2.999107197	-1.22808365	1.742410957
H	3.07687347	-1.241167948	2.818938993
C	-2.973744934	-2.403269731	1.36264486
H	-3.844135676	-2.682762771	1.939411225
C	-3.050914928	-2.372055664	-0.049829502
H	-3.982979658	-2.616150386	-0.539557203
C	4.130780262	-1.2031945	0.998162523
H	5.096472092	-1.188223814	1.483866396
C	4.057025112	-1.190738995	-0.414284382
H	4.965882675	-1.154774085	-0.998482757

References

(1) J. H. Golden, *J. Chem. Soc.* **1961**, 3741-3748.

(2) T. Nishiuchi, K. Kisaka, T. Kubo, *Angew. Chem. Int. Ed*. **2021**, *60*, 5400-5406.

(3) M. Ito, T. Fujino, L. Zhang, S. Yokomori, T. Higashino, R. Makiura, K. J. Takeno, T. Ozaki, H. Mori, *J. Am. Chem. Soc.* **2023**, *145*, 2127-2134.